SIAM J. NUMER. ANAL.
Vol. 58, No. 4, pp. 2294–2314

ON ENERGY STABLE, MAXIMUM-PRINCIPLE PRESERVING, SECOND-ORDER BDF SCHEME WITH VARIABLE STEPS FOR THE ALLEN–CAHN EQUATION*

HONG-LIN LIAO†, TAO TANG‡, AND TAO ZHOU§

Abstract. In this work, we investigate the two-step backward differentiation formula (BDF2) with nonuniform grids for the Allen–Cahn equation. We show that the nonuniform BDF2 scheme is energy stable under the time-step ratio restriction $r_k := \tau_k/\tau_{k-1} < (3+\sqrt{17})/2 \approx 3.561$. Moreover, by developing a novel kernel recombination and complementary technique, we show, for the first time, the discrete maximum bound principle of the BDF2 scheme under the time-step ratio restriction $r_k < 1+\sqrt{2} \approx 2.414$ and a practical time-step constraint. The second-order rate of convergence in the maximum norm is also presented. Numerical experiments are provided to support the theoretical findings.

Key words. Allen–Cahn equation, nonuniform BDF2 scheme, energy stability, discrete maximum principle, convergence analysis

AMS subject classifications. 35K35, 35K55, 65M12, 65M60

DOI. 10.1137/19M1289157

1. Introduction.

The phase field equations are important models in describing a host of free-boundary problems in various areas, including material, physical, and biology systems [1, 3, 13, 29]. Meanwhile, numerical schemes for phase field equations have also been extensively studied in recent years [5, 11, 12, 21, 28, 30]. The main focuses of the numerical schemes are the discrete energy stability (e.g., [4, 5, 24, 25, 28]) and the discrete maximum bound principle (for Allen–Cahn equations) [6, 14, 26], which are inherent properties in the continuous level. Another key feature of the phase field models is that the associate solutions in general admit multiple time scales; i.e., an initial dynamics evolves on a fast time scale and later coarsening evolves on a very slow time scale. This motivates the use of nonuniform meshes in time domain [8, 11, 16, 20, 23, 31]; i.e., one adopts small time steps for capturing the fast dynamics when the solution varies rapidly and uses large time steps otherwise to accelerate the time integration. While the numerical analysis for numerical schemes with uniform grids has been well investigated, the relevant analysis for nonuniform grids have not been well studied. In fact, even for linear/semilinear parabolic equations, the relevant

*Received by the editors September 23, 2019; accepted for publication (in revised form) May 20, 2020; published electronically August 12, 2020.
https://doi.org/10.1137/19M1289157
Funding: The work of the first author was supported by the NUAA Scientific Research Starting Fund of Introduced Talent grant 1008-56SYAH18037. The work of the second and third authors was partially supported by the National Natural Science Foundation of China grant 11731006 and the Science Challenge Project grant TZ2018001. The work of the third author was partially supported by the National Natural Science Foundation of China grants 11822111, 11688101, 11571351, the NCMIS, and the Youth Innovation Promotion Association (CAS).

†Department of Mathematics, Nanjing University of Aeronautics and Astronautics, Nanjing 211106, People's Republic of China (liaohl@nuaa.edu.cn).
‡SUSTech International Center for Mathematics, Shenzhen, China, and Division of Science and Technology, BNU-HKBU United International College, Zhuhai, Guangdong Province, China (tangt@sustech.edu.cn).
§NCMIS & LSEC, Institute of Computational Mathematics and Scientific/Engineering Computing, Academy of Mathematics and Systems Science, Chinese Academy of Sciences, Beijing, 100190, People's Republic of China (tzhou@lsec.cc.ac.cn).

study is far from complete [2, 7, 15].

To this end, we investigate in this work the well-known two-step backward differentiation formula (BDF2) [2, 7, 9, 10, 15, 22, 30] with nonuniform grid for the Allen–Cahn equation. As a simple phase field model, the Allen–Cahn equation admits the energy dissipation law and the maximum bound principle in the continuous level, and our purpose is to investigate whether the nonuniform BDF2 scheme can preserve these properties in the discrete level. Compared to existing literature, our contributions are threefold:

- We show that the nonuniform BDF2 scheme is energy stable under the time-step ratio restriction $r_k := \tau_k/\tau_{k-1} < (3+\sqrt{17})/2 \approx 3.561$.
- We show, for the first time, the discrete maximum bound principle of the nonuniform BDF2 scheme under the time-step ratio restriction $r_k < 1+\sqrt{2}$ and a practical time-step constraint.
- We show the second-order rate of convergence in the maximum norm and present several experiments to support the theoretical findings.

We mention a related work [4], where the nonuniform BDF2 scheme (combined with the convex splitting approach) is investigated for the Cahn–Hilliard equation, and the energy stability and convergence analysis are presented under similar time-step ratio restrictions as in the current work. The key tool in [4] for the optimal error estimates is a generalized discrete Gronwall inequality. In contrast, we develop in this work a novel kernels recombination and complement (KRC) technique for the analysis. Moreover, our proof for the discrete maximum bound principle of the nonuniform BDF2 scheme seems to be the first work with such results.

The rest of this paper is organized as follows. In section 2, we provide some preliminaries. The discrete maximum bound principle and the discrete energy stability are presented in sections 3 and 4, respectively. In section 5, we show the rigorous convergence analysis in the maximum norm, and this is followed by several numerical examples in section 6. We finally give some concluding remarks in section 7.

2. Preliminaries. We consider the following Allen–Cahn equation:

$$\partial_t u(\mathbf{x},t) = \varepsilon^2 \Delta u - f(u), \quad \mathbf{x}\in\Omega, \quad 0<t\le T, \tag{2.1}$$

$$u(\mathbf{x},0) = u_0(\mathbf{x}), \quad \mathbf{x}\in\bar{\Omega}, \tag{2.2}$$

where $\mathbf{x} = (x,y)^T$ and $\Omega = (0,L)^2$ with its closure $\bar{\Omega}$. The nonlinear bulk force $f(u)$ is given by $f(u) = u^3 - u$, and the small constant $0 < \varepsilon \ll 1$ is the interaction length that describes the thickness of the transition boundary between materials. For simplicity, we consider the periodic boundary conditions. As is well known, the above Allen–Cahn equation can be viewed as an L^2-gradient flow of the following Ginzburg–Landau free energy functional:

$$E[u](t) := \int_\Omega \Big(\frac{1}{2}\varepsilon^2|\nabla u|^2 + F[u]\Big)\,\mathrm{d}\mathbf{x}, \quad F[u] = \frac{1}{4}(1-u^2)^2. \tag{2.3}$$

In other words, the Allen–Cahn equation (2.1) admits the following energy dissipation law:

$$\frac{\mathrm{d}E}{\mathrm{d}t} \le 0. \tag{2.4}$$

Moreover, the following maximum bound principle holds:

$$|u(\mathbf{x},t)| \le 1 \quad \text{if} \quad |u(\mathbf{x},0)| \le 1. \tag{2.5}$$

2.1. The nonuniform BDF2 scheme. We consider a general nonuniform time grid $0 = t_0 < t_1 < t_2 < \cdots < t_N = T$ with the time step $\tau_k := t_k - t_{k-1}$ for $1 \le k \le N$ and the maximum step size $\tau := \max_{1\le k\le N} \tau_k$. For any time sequence $\{v^n\}_{n=0}^N$, we denote $\nabla_\tau v^n := v^n - v^{n-1}$ and $\partial_\tau v^n := \nabla_\tau v^n/\tau_n$. For $k = 1, 2$, let $\Pi_{n,k}v$ be the interpolating polynomial of a function v over $k+1$ nodes $t_{n-k}, \ldots, t_{n-1}$ and t_n. Then by taking $v^n = v(t_n)$, the BDF1 formula yields

$$D_1 v^n := (\Pi_{n,1}v)'(t) = \nabla_\tau v^n/\tau_n, \quad n \ge 1,$$

and furthermore, the well-known BDF2 formula reads

$$D_2 v^n := (\Pi_{n,2}v)'(t_n) = \frac{1+2r_n}{\tau_n(1+r_n)}\nabla_\tau v^n - \frac{r_n^2}{\tau_n(1+r_n)}\nabla_\tau v^{n-1}, \quad n \ge 2, \tag{2.6}$$

where the adjacent time-step ratios r_k are defined by $r_1 \equiv 0$ (if necessary) and

$$r_k := \frac{\tau_k}{\tau_{k-1}}, \quad 2 \le k \le N.$$

To introduce the fully discrete scheme, we consider a central finite difference approximation in the physical domain. For a positive integer M, let $h := L/M$ be the spatial grid length, and we set $\bar\Omega_h := \{\mathbf{x}_h = (ih, jh) \,|\, 0 \le i, j \le M\}$. For any grid function $\{v_h \,|\, \mathbf{x}_h \in \bar\Omega_h\}$, we denote

$$\mathbb{V}_h := \big\{v \,|\, v = (v_j)^T \ \text{ for } \ 1 \le j \le M, \ \text{ with } \ v_j = (v_{i,j})^T \ \text{ for } \ 1 \le i \le M\big\},$$

where v^T is the transpose of the vector v. We also define the associate maximum norm $\|v\|_\infty := \max_{\mathbf{x}_h\in\Omega_h} |v_h|$. We shall denote by Λ_h the discrete matrix of Laplace operator Δ subject to periodic boundary conditions.

In general, one can use the BDF1 scheme to obtain first-level solution u^1 by considering $D_2 v^1 := D_1 v^1$, as the BDF2 formula needs two starting values and the BDF1 scheme generates a second-order accurate solution at the first time grid. Then, we have the following fully discrete nonlinear BDF2 time-stepping scheme:

$$D_2 u^n = \varepsilon^2 \Lambda_h u^n - f(u^n), \quad n \ge 1, \tag{2.7}$$

where the vector $f(u^n)$ is defined elementwise, that is, $f(u^n) := (u^n)^{\cdot 3} - u^n$.

2.2. Summary of main contributions. The main purpose of this work is to analyze the nonuniform BDF2 scheme (2.7). In particular, we shall show in Theorem 3.1 in the next section that scheme (2.7) admits a discrete energy stability, under the following mild time-step ratio constraint:

S1. $0 < r_k < (3+\sqrt{17})/2 \approx 3.561, \ 2 \le k \le N$.

Then, we present the discrete maximum bound principle and convergence estimates of scheme (2.7) in section 4. To do this, we shall propose a novel kernels recombination and complement (KRC) technique. More precisely, the BDF2 formula (2.6) is first regarded as a discrete convolution summation,

$$D_2 v^n = \sum_{k=1}^n b_{n-k}^{(n)} \nabla_\tau v^k, \quad n \ge 1, \tag{2.8}$$

where the discrete convolution kernels $b_{n-k}^{(n)}$ are defined by $b_0^{(1)} := 1/\tau_1$ and

$$b_0^{(n)} := \frac{1+2r_n}{\tau_n(1+r_n)}, \quad b_1^{(n)} := -\frac{r_n^2}{\tau_n(1+r_n)}, \quad \text{and} \quad b_j^{(n)} := 0 \ \text{ for } \ 2 \le j \le n. \tag{2.9}$$

For notational simplicity, we set $b_n^{(n)} := 0$ for $n \geq 1$ when necessary, and we set $\sum_{k=i}^{j} \cdot = 0$ if the index $i > j$.

In the *kernels recombination stage* of the KRC, we introduce a new class of variables $\{\bar{v}^k\}$ that consists of a linear combination of the original variables $\{v^k\}$ and reformulates $D_2 v^n$ into a new discrete convolution form, such as $\sum_{k=1}^{n} d_{n-k}^{(n)} \nabla_\tau \bar{v}^k$, which always involves all of previous solutions $\{\bar{v}^k\}_{k=0}^{n-1}$. The main aim is to build a new class of discrete convolution kernels $d_j^{(n)}$ so that they are nonnegative and monotonously decreasing. Then we show in Theorem 4.1 in section 4 that the scheme (2.7) preserves the maximum bound principle under a time-step ratio restriction that coincides with the zero-stability condition due to Grigorieff [10]:

S0. $0 < r_k < 1 + \sqrt{2} \approx 2.414$ for $2 \leq k \leq N$.

The discrete maximum bound principle offers us the possibility to show the maximum norm convergence without any Lipschitz assumptions on the nonlinear bulk force. With the help of the *kernels complementary stage* of the KRC, we build in Lemma 5.1 a new discrete Grönwall inequality. Then we show in Theorem 5.1 that the scheme (2.7) is of second-order convergence in the maximum norm under the step-ratio condition **S0**. To the best of our knowledge, it is the *first* work establishing such convergence results for the nonuniform BDF2 scheme under the Grigorieff zero-stability condition **S0**.

3. Solvability and energy stability. We first list some well-known properties of the matrix Λ_h in the following lemma.

LEMMA 3.1. *The discrete matrix Λ_h of Laplace operator Δ has the following properties:*

(a) *The discrete matrix Λ_h is symmetric.*
(b) *For any nonzero $v \in \mathbb{V}_h$, $v^T \Lambda_h v \leq 0$, i.e., the matrix Λ_h is negative semidefinite.*
(c) *The elements of $\Lambda_h = (d_{ij})$ fulfill $d_{ii} = -\max_i \sum_{j \neq i} |d_{ij}|$ for each i.*

Then, we show the solvability of scheme (2.7) in the following lemma.

LEMMA 3.2. *The discrete scheme* (2.7) *is uniquely solvable if*

$$\tau_n < \frac{1 + 2r_n}{1 + r_n}, \quad n \geq 1.$$

Notice that the above step constraint is practical as it is sufficient to require $\tau_n < 1$.

Proof. We rewrite the nonlinear scheme (2.7) as

$$G_h u^n + (u^n)^{\cdot 3} = g(u^{n-1}) \quad \text{with} \quad g(u^{n-1}) := b_0^{(n)} u^{n-1} - b_1^{(n)} \nabla_\tau u^{n-1}, \quad n \geq 1,$$

where $G_h := b_0^{(n)} - 1 - \varepsilon^2 \Lambda_h$. If the time-step size $\tau_n < \frac{1+2r_n}{1+r_n}$, by definition (2.9) we have $b_0^{(n)} > 1$. Thus the matrix G_h is positive definite according to Lemma 3.1(b). Consequently, the solution of nonlinear equations solves

$$u^n = \arg \min_{w \in \mathbb{V}_h} \left\{ \frac{1}{2} w^T G_h w + \frac{1}{4} \sum_{k=1}^{M} w_k^4 - w^T g(u^{n-1}) \right\}, \quad n \geq 1.$$

The strict convexity of the above objective function implies the unique solvability of (2.7). ∎

We now consider the energy stability of the nonuniform BDF2 scheme (2.7) by defining a modified discrete energy $\widehat{E}$:

$$\widehat{E}[u^k] := E[u^k] + \frac{r_{k+1}\tau_k}{2(1+r_{k+1})}\sum_{i=1}^{M}\big(\partial_\tau u_i^k\big)^2, \quad k \ge 1, \tag{3.1}$$

where we set $\widehat{E}[u^0] = E[u^0]$, which corresponds to the setting $r_1 \equiv 0$, and $E[u^k]$ is the original discrete energy that is given by

$$E[u^k] := -\frac{\varepsilon^2}{2}(u^k)^T\Lambda_h u^k + \frac{1}{4}\sum_{i=1}^{M}\big(1-(u_i^k)^2\big)^2, \quad k \ge 0.$$

Notice that the modified energy $\widehat{E}[u^k] \to E[u^k]$ when $\tau \to 0$. We are now ready to present the following energy stability of scheme (2.7).

THEOREM 3.1. *Assume that the step-ratio condition* **S1** *holds, and moreover, suppose that*

$$\tau_k \le \min\left\{\frac{1+2r_k}{1+r_k}, \frac{2+4r_k-r_k^2}{1+r_k} - \frac{r_{k+1}}{1+r_{k+1}}\right\} \quad \textit{for } k \ge 1. \tag{3.2}$$

Then, the discrete solution u^n of the BDF2 time-stepping scheme (2.7) *satisfies*

$$\widehat{E}[u^k] \le \widehat{E}[u^{k-1}], \quad k \ge 1. \tag{3.3}$$

Proof. Taking the L^2 inner product (in the vector space) of (2.7) with $(\nabla_\tau u^n)^T$, we have

$$\sum_{i=1}^{M} D_2 u_i^n\big(\nabla_\tau u_i^n\big) - \varepsilon^2(\nabla_\tau u^n)^T\Lambda_h u^n + \sum_{i=1}^{M} f(u_i^n)\nabla_\tau u_i^n = 0, \quad n \ge 1. \tag{3.4}$$

By using Lemma 3.1(a)–(b), one gets

$$\begin{aligned}-\varepsilon^2(\nabla_\tau u^n)^T\Lambda_h u^n &= -\frac{\varepsilon^2}{2}(u^n)^T\Lambda_h u^n + \frac{\varepsilon^2}{2}(u^{n-1})^T\Lambda_h u^{n-1} - \frac{\varepsilon^2}{2}(\nabla_\tau u^n)^T\Lambda_h\big(\nabla_\tau u^n\big)\\ &\ge -\frac{\varepsilon^2}{2}(u^n)^T\Lambda_h u^n + \frac{\varepsilon^2}{2}(u^{n-1})^T\Lambda_h u^{n-1}.\end{aligned}$$

It is easy to check the following identity:

$$4\left(a^3-a\right)(a-b) + 2(1-a^2)(a-b)^2 = (1-a^2)^2 - (1-b^2)^2 + (a^2-b^2)^2.$$

Taking $a := u_i^n$ and $b := u_i^{n-1}$ in the above equality, we obtain

$$\begin{aligned}\sum_{i=1}^{M} f(u_i^n)\big(\nabla_\tau u_i^n\big) &= \sum_{i=1}^{M}\big((u_i^n)^3 - u_i^n\big)\big(\nabla_\tau u_i^n\big)\\ &\ge \frac{1}{4}\sum_{i=1}^{M}\big(1-(u_i^n)^2\big)^2 - \frac{1}{4}\sum_{i=1}^{M}\big(1-(u_i^{n-1})^2\big)^2 - \frac{1}{2}\sum_{i=1}^{M}\big(\nabla_\tau u_i^n\big)^2.\end{aligned}$$

Thus it follows from (3.4) that

$$\sum_{i=1}^{M} D_2 u_i^n \big(\nabla_\tau u_i^n\big) - \frac{\tau_n^2}{2} \sum_{i=1}^{M} \big(\partial_\tau u_i^n\big)^2 + E(u^n) \le E(u^{n-1}), \quad n \ge 1. \tag{3.5}$$

We now consider the mathematical induction argument. For the case of $n = 1$, we have

$$\begin{aligned} D_2 u_i^1 \big(\nabla_\tau u_i^1\big) &= D_1 u_i^1 \big(\nabla_\tau u_i^1\big) = \frac{r_2 \tau_1}{2(1+r_2)} \big(\partial_\tau u_i^1\big)^2 + \frac{2+r_2}{2(1+r_2)} \tau_1 \big(\partial_\tau u_i^1\big)^2 \\ &\ge \frac{r_2 \tau_1}{2(1+r_2)} \big(\partial_\tau u_i^1\big)^2 + \frac{\tau_1^2}{2} \big(\partial_\tau u_i^1\big)^2, \end{aligned}$$

where the condition (3.2) of $k = 1$ was used in the last inequality. The estimate (3.5) then gives

$$\widehat{E}[u^1] \le \widehat{E}[u^0] = E[u^0].$$

For the general case of $n \ge 2$, we use the identity $2a(a-b) = a^2 - b^2 + (a-b)^2$ and the definition (2.9) of BDF2 kernels to obtain

$$\begin{aligned} D_2 u_i^n \big(\nabla_\tau u_i^n\big) &= \big(b_0^{(n)} + b_1^{(n)}\big) \big(\nabla_\tau u_i^n\big)^2 - b_1^{(n)} \big(\nabla_\tau u_i^n - \nabla_\tau u_i^{n-1}\big) \nabla_\tau u_i^n \\ &= \big(b_0^{(n)} + \frac{1}{2} b_1^{(n)}\big) \big(\nabla_\tau u_i^n\big)^2 + \frac{1}{2} b_1^{(n)} \big(\nabla_\tau u_i^{n-1}\big)^2 - \frac{1}{2} b_1^{(n)} \big(\nabla_\tau u_i^n - \nabla_\tau u_i^{n-1}\big)^2 \\ &\ge \big(b_0^{(n)} + \frac{1}{2} b_1^{(n)}\big) \big(\nabla_\tau u_i^n\big)^2 + \frac{1}{2} b_1^{(n)} \big(\nabla_\tau u_i^{n-1}\big)^2 \\ &= \frac{r_{n+1} \tau_n}{2(1+r_{n+1})} \big(\partial_\tau u_i^n\big)^2 - \frac{r_n \tau_{n-1}}{2(1+r_n)} \big(\partial_\tau u_i^{n-1}\big)^2 \\ &\quad + \Big(\frac{2+4r_n - r_n^2}{1+r_n} - \frac{r_{n+1}}{1+r_{n+1}}\Big) \frac{\tau_n}{2} \big(\partial_\tau u_i^n\big)^2. \end{aligned}$$

Inserting this estimate into (3.5), we obtain

$$\Big(\frac{2+4r_n - r_n^2}{1+r_n} - \frac{r_{n+1}}{1+r_{n+1}} - \tau_n\Big) \frac{\tau_n}{2} \sum_{i=1}^{M} \big(\partial_\tau u_i^n\big)^2 + \widehat{E}[u^n] \le \widehat{E}[u^{n-1}], \quad 2 \le n \le N.$$

The desired result follows by noticing the restriction (3.2), and this completes the proof. ∎

Some comments for the time-step restriction (3.2) are listed below. The first constraint in (3.2) comes from Lemma 3.2 for solvability, and it suffices to choose $\tau_k \le 1$ to ensure it for any $r_k > 0$.

It remains to check the second constraint in (3.2). For $n = 1$, the constraint (3.2) yields $\tau_1 \le \frac{2+r_2}{1+r_2}$ and one can also simply choose $\tau_1 \le 1$. Under the condition **S1**, one has $0 < r_k < r_s$, where $r_s = \frac{3+\sqrt{17}}{2}$ is the positive root of the algebraic equation $2 + 3r_s - r_s^2 = 0$, and $\frac{r_{k+1}}{1+r_{k+1}} < \frac{r_s}{1+r_s} = \frac{\sqrt{17}-1}{4} \approx 0.78$. So the time-step restriction (3.2) is fulfilled by choosing

$$\tau_k \le \frac{2+4r_k - r_k^2}{1+r_k} - \frac{r_s}{1+r_s} = \frac{2+4r_k - r_k^2}{1+r_k} - \frac{\sqrt{17}-1}{4} \quad \text{for } k \ge 2.$$

Actually, let $h(x) := \frac{2+4x-x^2}{1+x}$ such that $h'(x) = \frac{x+1+\sqrt{3}}{(1+x)^2}(\sqrt{3} - 1 - x)$. We consider three cases:

(i) If $0 < r_k \le \sqrt{3}-1$, then $h'(r_k) \ge 0$ and $h(r_k) \ge h(0) = 2$. One can choose time steps $\tau_k \le \min\{1, \frac{9-\sqrt{17}}{4}\} = 1$ to ensure (3.2).

(ii) If $\sqrt{3}-1 < r_k \le \sqrt{2}+1$, then $h'(r_k) < 0$ and $h(r_k) \ge h(\sqrt{2}+1) = 1+\frac{\sqrt{2}}{2}$. One can choose time steps $\tau_k \le 1+\frac{\sqrt{2}}{2}-\frac{\sqrt{17}-1}{4} \approx 0.93$ to ensure (3.2).

(iii) If $\sqrt{2}+1 < r_k < r_s$, then $h'(r_k) < 0$ and $h(r_k) > h(r_s) = \frac{r_s}{1+r_s}$. In this case, especially when the current step ratio $r_k \to r_s$, one can choose a small time step τ_{k+1} or step ratio r_{k+1} to ensure the time-step restriction (3.2) in adaptive computations. As an example, the time steps $\tau_k \le \frac{1}{2}$ are sufficient if one chooses the next step ratio $r_{k+1} \le \frac{2h(r_s)-1}{3-2h(r_s)} \approx 0.39$.

To summarize, under the condition **S1**, the time-step size constraint (3.2) is reasonable. In particular, it is practical in controlling the next time step τ_{k+1} in adaptive simulations.

4. Kernels recombination and discrete maximum bound principle. In this section, we shall show the discrete maximum bound principle of scheme (2.7).

4.1. Reformation of BDF2 formula. We first introduce a new class of variables below (see [18, Remark 6] for technical motivations):

$$\bar{v}^0 := v^0 \quad \text{and} \quad \bar{v}^k := v^k - \eta v^{k-1} \ \text{ for } k \ge 1, \tag{4.1}$$

where η is a real parameter to be determined. It is easy to find the substitution formula

$$v^k = \bar{v}^k + \eta v^{k-1} = \bar{v}^k + \eta\big(\bar{v}^{k-1} + \eta v^{k-2}\big) = \cdots = \sum_{\ell=0}^{k} \eta^{k-\ell}\bar{v}^\ell \quad \text{for } k \ge 1, \tag{4.2}$$

and then we have

$$\nabla_\tau v^k = \sum_{\ell=1}^{k} \eta^{k-\ell}\nabla_\tau \bar{v}^\ell + \eta^k v^0 \quad \text{for } k \ge 1.$$

By inserting the above equation into (2.8) and exchanging the summation order, we obtain an updated BDF2 formula,

$$D_2 v^n \equiv \sum_{j=1}^{n} d_{n-j}^{(n)} \nabla_\tau \bar{v}^j + d_n^{(n)} \bar{v}^0 \quad \text{for } n \ge 1, \tag{4.3}$$

where the new discrete convolution kernels $d_{n-j}^{(n)}$ can be defined by

$$d_{n-j}^{(n)} := \sum_{k=j}^{n} b_{n-k}^{(n)} \eta^{k-j} \quad \text{for } 1 \le j \le n, \quad \text{and} \quad d_n^{(n)} := \eta d_{n-1}^{(n)}.$$

Alternatively, we have the following explicit formula:

$$d_0^{(n)} := b_0^{(n)} \quad \text{and} \quad d_j^{(n)} := \eta^{j-1}\big(b_0^{(n)}\eta + b_1^{(n)}\big) \quad \text{for } 1 \le j \le n. \tag{4.4}$$

We shall require that the new discrete kernels $d_{n-j}^{(n)}$ are nonnegative and decreasing, that is, $d_0^{(n)} \ge d_1^{(n)} \ge \cdots \ge d_n^{(n)} \ge 0$. By the definitions (4.4) and (2.9), it is easy to check that this aim can be achieved by setting

$$\frac{r_k^2}{1+2r_k} \le \eta < 1 \quad \text{for } k \ge 2. \tag{4.5}$$

Meanwhile, we require that the adjacent time-step ratios satisfy the condition **S0**, that is, $r_k < 1 + \sqrt{2}$, which coincides with the Grigorieff zero-stability condition [10] for ODE problems.

Now, by using the new formula (4.3), the numerical scheme (2.7) reads

$$\sum_{j=1}^{n} d_{n-j}^{(n)} \nabla_\tau \bar{u}^j + d_n^{(n)} \bar{u}^0 = \varepsilon^2 \Lambda_h u^n - f(u^n) \quad \text{for } n \geq 1. \tag{4.6}$$

This equation will be our starting point to establish the discrete maximum bound principle. Recalling the definition of $\bar{u}^j$ and the substitution formula (4.2), we have

$$\begin{aligned} \big(d_0^{(n)} - 1 - \varepsilon^2 \Lambda_h\big) u^n + (u^n)^{\cdot 3} &= \eta d_0^{(n)} u^{n-1} + \sum_{j=0}^{n-1} \big(d_{n-j-1}^{(n)} - d_{n-j}^{(n)}\big) \bar{u}^j \\ &= d_0^{(n)} \sum_{j=0}^{n-1} \eta^{n-j} \bar{u}^j + \sum_{j=0}^{n-1} \big(d_{n-j-1}^{(n)} - d_{n-j}^{(n)}\big) \bar{u}^j \quad \text{for } n \geq 1. \end{aligned} \tag{4.7}$$

This formulation (4.7) will be used to evaluate u^n by using the information from $\{\bar{u}^j\}_{j=0}^{n-1}$. Again, we apply the substitution formula (4.2) to derive from (4.6) that

$$\begin{aligned} \big(d_0^{(n)} + S_n - \varepsilon^2 \Lambda_h\big) \bar{u}^n &= \sum_{j=0}^{n-1} \big(d_{n-j-1}^{(n)} - d_{n-j}^{(n)} - S_n \eta^{n-j} + \eta^{n-j} \varepsilon^2 \Lambda_h\big) \bar{u}^j \\ &\quad + (S_n + 1) u^n - (u^n)^{\cdot 3} \\ &= \sum_{j=0}^{n-1} Q_{n-j}^{(n)} \bar{u}^j + (S_n + 1) u^n - (u^n)^{\cdot 3} \quad \text{for } n \geq 1, \end{aligned} \tag{4.8}$$

where S_n is a real parameter (that can depend on the time-levels) to be determined, and the matrix

$$Q_j^{(n)} := \big(d_{j-1}^{(n)} - d_j^{(n)} - S_n \eta^j\big) I + \eta^j \varepsilon^2 \Lambda_h \quad \text{for } 1 \leq j \leq n. \tag{4.9}$$

This formulation will be used to evaluate $\bar{u}^n$ by using the information $\{\bar{u}^j\}_{j=0}^{n-1}$ and u^n.

4.2. Choice of recombined parameter. The next lemma presents a time-step size restriction so that the matrix $Q_j^{(n)}$ in (4.9) is bounded in the maximum norm.

LEMMA 4.1. *Assume that the step-ratio condition* **S0** *holds, and suppose that the time-step size satisfies*

$$\tau_n \leq \frac{(1 + 2r_n)\eta - r_n^2}{\eta^2 (1 + r_n)} \frac{1 - \eta}{S_n + 4\varepsilon^2 h^{-2}} \quad \textit{for } n \geq 1, \tag{4.10}$$

where the recombined parameter η *satisfies* (4.5). *Then the matrix* $Q_j^{(n)}$ *in* (4.9) *fulfills*

$$\big\| Q_j^{(n)} \big\|_\infty \leq d_{j-1}^{(n)} - d_j^{(n)} - S_n \eta^j \quad \textit{for } 1 \leq j \leq n. \tag{4.11}$$

Proof. Consider the case of $n \geq 2$. By the definition (4.4), the matrix $Q_j^{(n)}$ in (4.9) reads

$$Q_j^{(n)} = \eta^j \left[(1-\eta)\eta^{-2}\big(b_0^{(n)}\eta + b_1^{(n)}\big) - S_n\right] I + \eta^j \varepsilon^2 \Lambda_h \quad \text{for } 2 \leq j \leq n.$$

The time-step condition (4.10) together with the definition (2.9) yields

$$\frac{1-\eta}{\eta^2}\big(b_0^{(n)}\eta + b_1^{(n)}\big) - S_n \geq \frac{4\varepsilon^2}{h^2}.$$

Thus all the elements of the matrix $Q_j^{(n)} = \big(q_{k\ell}^{(n,j)}\big)$ are nonnegative and

$$\big\|Q_j^{(n)}\big\|_\infty = \max_k \sum_\ell \big|q_{k\ell}^{(n,j)}\big| = \max_k \sum_\ell q_{k\ell}^{(n,j)} \leq d_{j-1}^{(n)} - d_j^{(n)} - S_n\eta^j \quad \text{for } 2 \leq j \leq n.$$

The desired estimate (4.11) holds for $2 \leq j \leq n$. It remains to consider the case $j = 1$ for $n \geq 1$. By using the step condition (4.10), the definitions (2.9) and (4.4) show that (with $r_1 = 0$)

$$\begin{aligned} d_0^{(n)} - d_1^{(n)} - S_n\eta &= (1-\eta)b_0^{(n)} - b_1^{(n)} - S_n\eta \\ &= \eta^{-1}\big[(1-\eta)\big(b_0^{(n)}\eta + b_1^{(n)}\big) - b_1^{(n)} - S_n\eta^2\big] \\ &\geq \eta\Big[(1-\eta)\eta^{-2}\big(b_0^{(n)}\eta + b_1^{(n)}\big) - S_n\Big] \geq \frac{4\eta\varepsilon^2}{h^2}. \end{aligned}$$

Thus, all elements of the matrix $Q_1^{(n)} = \big(q_{k\ell}^{(n,1)}\big)$ are nonnegative and

$$\big\|Q_1^{(n)}\big\|_\infty = \max_k \sum_\ell \big|q_{k\ell}^{(n,1)}\big| = \max_k \sum_\ell q_{k\ell}^{(n,1)} \leq d_0^{(n)} - d_1^{(n)} - S_n\eta.$$

The proof is complete. ∎

Further comments for the restriction (4.10) are listed below. We set

$$K(\eta) := \frac{1-\eta}{\eta^2}\frac{(1+2r_n)\eta - r_n^2}{1+r_n}.$$

Obviously, $K(\eta) > 0$ if the parameter η satisfies (4.5). Moreover, $K'(\eta) = \frac{1+r_n}{\eta^3}\big(\frac{2r_n^2}{(1+r_n)^2} - \eta\big)$, and $K(\eta)$ approaches its maximum value when $\eta \to \frac{2r_n^2}{(1+r_n)^2}$. For a fixed maximum step ratio $r_s \in [1, 1+\sqrt{2})$, one can choose the parameter $\eta \in \big[\frac{r_s^2}{1+2r_s}, 1\big)$ such that the condition (4.5) holds at any time level. To relieve the restriction (4.10) on the time-step size, we can choose in all of the above derivations

$$\eta := \frac{2r_s^2}{(1+r_s)^2} \quad \text{with } r_s \in [1, 1+\sqrt{2}). \tag{4.12}$$

For example, consider the uniform mesh case with $r_n = r_s = 1$; one can take $\eta = \frac{1}{2}$ so that the time-step condition (4.10) reads

$$\tau_n = \tau \leq \frac{1}{2(S_n + 4\varepsilon^2 h^{-2})}.$$

Consider the case of $r_s = 2$; one can take the recombined parameter $\eta = 8/9$ so that the time-step condition (4.10) requires

$$\tau_n \le \frac{1}{48}\frac{1}{S_n + 4\varepsilon^2 h^{-2}}.$$

The time-step condition (4.10) with $S_n = 2$ will be used to establish the discrete maximum bound principle in the next subsection.

4.3. Discrete maximum bound principle. To establish the discrete maximum-principle, we recall the following result [14, Lemma 3.2].

LEMMA 4.2. *Let B be a real $M \times M$ matrix and $A = aI - B$ with $a > 0$. If the elements of $B = (b_{ij})$ fulfill $b_{ii} = -\max_i \sum_{j\neq i} |b_{ij}|$, then for any $c > 0$ and $V \in \mathbb{R}^M$ we have*

$$\|AV\|_\infty \ge a\|V\|_\infty \quad \text{and} \quad \|AV + c(V)^3\|_\infty \ge a\|V\|_\infty + c\|V\|_\infty^3.$$

We are now ready to present the following theorem on the discrete maximum bound principle.

THEOREM 4.1. *Assume that the step-ratio restriction* **S0** *holds and suppose that the time-step size satisfies*

$$\tau_n \le \frac{(1+2r_n)\eta - r_n^2}{\eta^2(1+r_n)}\frac{1-\eta}{2+4\varepsilon^2 h^{-2}} \quad \text{for } n \ge 1, \tag{4.13}$$

where the recombined parameter η is defined by (4.12)*. Then, the BDF2 time-stepping scheme* (2.7) *preserves the maximum bound principle at the discrete level, that is,*

$$\|u^k\|_\infty \le 1 \ \text{ for } 1 \le k \le N \quad \text{if } \ \|u^0\|_\infty \le 1.$$

Proof. The desired result is a by-product of the following claim:

$$\|\bar{u}^k\|_\infty \le 1 - \eta \ \text{ for } 1 \le k \le N \quad \text{if } \ \|\bar{u}^0\|_\infty \le 1.$$

We now verify this new claim with the complete mathematical induction argument. Taking $n = 1$ in (4.7), one has

$$\big(d_0^{(1)} - 1 - \varepsilon^2\Lambda_h\big)u^1 + (u^1)^{\cdot 3} = \eta d_0^{(1)}u^0 + (1-\eta)d_0^{(1)}\bar{u}^0 = d_0^{(1)}\bar{u}^0.$$

Since $d_0^{(1)} = b_0^{(n)} > 1$, we apply Lemmas 3.1 and 4.2 to get

$$\big(d_0^{(1)} - 1\big)\|u^1\|_\infty + \|u^1\|_\infty^3 \le \big\|\big(d_0^{(1)} - 1 - \varepsilon^2\Lambda_h\big)u^1 + (u^1)^{\cdot 3}\big\|_\infty \le d_0^{(1)},$$

which implies $\|u^1\|_\infty \le 1$. To see this, notice that the function $g_c(z) := (c-1)\,z + z^3 - c$ is increasing with respect to $z > 0$ if the real parameter $c \ge 1$. So this contradicts with $\|u^1\|_\infty > 1$.

Next we shall bound $\|\bar{u}^1\|_\infty$. Because $|(c+1)z - z^3| \le c$ for $|z| \le 1$ if the real parameter $c \ge 2$, one has $\|3u^1 - (u^1)^{\cdot 3}\|_\infty \le 2$. Thus we take $n = 1$ and $S_1 = 2$ in the equation (4.8) and apply Lemma 4.1 to get

$$\begin{aligned}\big(d_0^{(1)} + 2\big)\|\bar{u}^1\|_\infty &\le \big\|\big(d_0^{(1)} + 2 - \varepsilon^2\Lambda_h\big)\bar{u}^1\big\|_\infty = \big\|Q_1^{(1)}\bar{u}^0 + 3u^1 - (u^1)^{\cdot 3}\big\|_\infty \\ &\le \|Q_1^{(1)}\|_\infty\|\bar{u}^0\|_\infty + \|3u^1 - (u^1)^{\cdot 3}\|_\infty \\ &\le d_0^{(1)} - d_1^{(1)} - 2\eta + 2 = (1-\eta)\big(d_0^{(1)} + 2\big),\end{aligned}$$

which yields $\|\bar{u}^1\|_\infty \le 1-\eta$.

For the general case of $2 \le n \le N$, assume that

$$\|\bar{u}^k\|_\infty \le 1-\eta \quad \text{for } 1 \le k \le n-1. \tag{4.14}$$

From the equation (4.7) and the expressions in (4.4), one applies Lemmas 3.1 and 4.2 to find

$$\begin{aligned}
\big(d_0^{(n)}-1\big)\|u^n\|_\infty + \|u^n\|_\infty^3 &\le \big\|\big(d_0^{(n)}-1-\varepsilon^2\Lambda_h\big)u^n + (u^n)^{\cdot 3}\big\|_\infty \\
&\le d_0^{(n)}\sum_{j=0}^{n-1}\eta^{n-j}\|\bar{u}^j\|_\infty + \sum_{j=0}^{n-1}\big(d_{n-j-1}^{(n)}-d_{n-j}^{(n)}\big)\|\bar{u}^j\|_\infty \\
&\le \eta d_0^{(n)} + (1-\eta)\big(d_0^{(n)}-d_{n-1}^{(n)}\big) + \big(d_{n-1}^{(n)}-d_n^{(n)}\big) = d_0^{(n)},
\end{aligned}$$

where the inductive hypothesis (4.14) and the identity $(1-\eta)\sum_{j=1}^{n-1}\eta^{n-j}+\eta^n=\eta$ have been used in the third inequality. This yields immediately

$$\|u^n\|_\infty \le 1. \tag{4.15}$$

It remains to evaluate $\|\bar{u}^n\|_\infty$. The above estimate (4.15) gives

$$\big\|3u^n-(u^n)^{\cdot 3}\big\|_\infty \le 2.$$

Now we take $S_n=2$ in the equation (4.8). By applying Lemma 4.1 and the inductive hypothesis (4.14) one has

$$\begin{aligned}
\big(d_0^{(n)}+2\big)\|\bar{u}^n\|_\infty &\le \sum_{j=0}^{n-1}\|Q_{n-j}^{(n)}\|_\infty\|\bar{u}^j\|_\infty + \big\|3u^n-(u^n)^{\cdot 3}\big\|_\infty \\
&\le (1-\eta)\sum_{j=1}^{n-1}\big(d_{n-j-1}^{(n)}-d_{n-j}^{(n)}-2\eta^{n-j}\big) + \big(d_{n-1}^{(n)}-d_n^{(n)}-2\eta^n\big)+2 \\
&= (1-\eta)\big(d_0^{(n)}-d_{n-1}^{(n)}\big) + \big(d_{n-1}^{(n)}-d_n^{(n)}\big) - 2(1-\eta)\sum_{j=1}^{n-1}\eta^{n-j} - 2\eta^n + 2 \\
&= (1-\eta)\big(d_0^{(n)}+2\big).
\end{aligned}$$

This leads to $\|\bar{u}^n\|_\infty \le 1-\eta$, and the proof is complete. ∎

Notice that in the Allen–Cahn equation (2.1), the coefficient $\varepsilon \ll 1$ represents the width of the diffusive interface. In practice, one should choose a small spatial step $h=\mathcal{O}(\varepsilon)$ to track the moving interface. Then the restriction (4.13) is approximately equivalent to

$$\tau_n \le \frac{(1+2r_n)\eta - r_n^2}{\eta^2(1+r_n)}\frac{1-\eta}{6} \quad \text{for } \eta := \frac{2r_s^2}{(1+r_s)^2} \quad \text{and} \quad n \ge 1.$$

On the other hand, the parameter η is introduced only for the theoretical analysis but is not necessary in numerical computations; thus the time-step restriction (4.13) seems to be rather practical. We also remark that Theorem 4.1 seems to be the first result on the second-order maximum-principle preserving scheme with variable steps.

5. Complementary kernels and convergence analysis. This section is devoted to convergence analysis. To this end, we introduce a class of discrete complementary convolution kernels $\{(Q_d)_{n-j}^{(n)}\}_{j=1}^{n}$ via the discrete kernels $d_j^{(n)}$ in (4.4),

(5.1)
$$(Q_d)_0^{(n)} := \frac{1}{d_0^{(n)}} \quad \text{and} \quad (Q_d)_{n-j}^{(n)} := \sum_{k=j+1}^{n} \frac{d_{k-j-1}^{(k)} - d_{k-j}^{(k)}}{d_0^{(j)}} (Q_d)_{n-k}^{(n)} \quad \text{for } 1 \le j \le n-1.$$

This type of discrete kernel was first introduced in [17] for numerical approximation of fractional Caputo derivatives and further generalized in [18] for more general discrete kernels. It is easy to check that the following complementary identity holds:

$$\sum_{j=k}^{n} (Q_d)_{n-j}^{(n)} d_{j-k}^{(j)} \equiv 1 \quad \forall\, 1 \le k \le n. \tag{5.2}$$

From the definition (4.4), we know that $d_j^{(n)}$ are nonnegative and decreasing. So the definition (5.1) implies that $(Q_d)_{n-j}^{(n)} \ge 0$. The identity (5.2) yields immediately

$$0 < (Q_d)_{n-j}^{(n)} \le \frac{1}{d_0^{(j)}} \qquad \forall\, 1 \le j \le n. \tag{5.3}$$

Now we apply the discrete complementary convolution kernels $\{(Q_d)_{n-j}^{(n)}\}_{j=1}^{n}$ and their properties (5.2)–(5.3) to build a novel discrete Grönwall lemma, which will play an important role in the analysis of the nonuniform BDF2 scheme.

LEMMA 5.1. *For constants $\kappa > 0$, $\lambda \in (0,1)$ and for any nonnegative sequences $\{g^k\}_{k=1}^{N}$ and $\{w^k\}_{k=0}^{N}$ such that*

$$\sum_{k=1}^{n} d_{n-k}^{(n)} \nabla_\tau w^k \le \kappa \sum_{k=1}^{n} \lambda^{n-k} w^k + g^n \quad \textit{for } 1 \le n \le N,$$

where the discrete kernels $d_j^{(n)}$ are defined by (4.4), if $b_0^{(n)} \ge 2\kappa$, then

$$w^n \le 2 \exp\big(\frac{2\kappa t_n}{1-\lambda}\big) \Big(w^0 + \sum_{j=1}^{n} \frac{g^j}{b_0^{(j)}} \Big) \quad \textit{for } 1 \le n \le N.$$

Proof. We have

$$\sum_{k=1}^{j} d_{j-k}^{(j)} \nabla_\tau w^k \le \kappa \sum_{k=1}^{j} \lambda^{j-k} w^k + g^j \quad \text{for } 1 \le j \le N.$$

Multiplying the above inequality by the complementary kernels $(Q_d)_{n-j}^{(n)}$ and taking the index j from 1 to n, one gets

$$\sum_{j=1}^{n} (Q_d)_{n-j}^{(n)} \sum_{k=1}^{j} d_{j-k}^{(j)} \nabla_\tau w^k \le \kappa \sum_{j=1}^{n} (Q_d)_{n-j}^{(n)} \sum_{k=1}^{j} \lambda^{j-k} w^k + \sum_{j=1}^{n} (Q_d)_{n-j}^{(n)} g^j.$$

By exchanging the summation order and applying the complementary identity (5.2), one has

$$\sum_{j=1}^{n}(Q_d)_{n-j}^{(n)}\sum_{k=1}^{j}d_{j-k}^{(j)}\nabla_\tau w^k=\sum_{k=1}^{n}\nabla_\tau w^k\sum_{j=k}^{n}(Q_d)_{n-j}^{(n)}d_{j-k}^{(j)}=w^n-w^0,$$
$$\sum_{j=1}^{n}(Q_d)_{n-j}^{(n)}\sum_{k=1}^{j}\lambda^{j-k}w^k=\sum_{k=1}^{n}w^k\sum_{j=k}^{n}(Q_d)_{n-j}^{(n)}\lambda^{j-k}.$$

Thus it follows that

$$w^n\le w^0+\kappa w^n(Q_d)_0^{(n)}+2\kappa\sum_{k=1}^{n-1}w^k\sum_{j=k}^{n}(Q_d)_{n-j}^{(n)}\lambda^{j-k}+\sum_{j=1}^{n}(Q_d)_{n-j}^{(n)}g^j\quad\text{for } 1\le n\le N.$$

Furthermore, the estimate (5.3) and the definition (4.4) yield

$$(Q_d)_{n-1}^{(n)}\le\frac{1}{b_0^{(1)}}=\tau_1\quad\text{and}\quad(Q_d)_{n-j}^{(n)}\le\frac{1}{b_0^{(j)}}=\frac{1+r_j}{1+2r_j}\tau_j\le\tau_j\quad\text{for } 2\le j\le n.$$

Setting $b_0^{(n)}\ge 2\kappa$ so that $(Q_d)_0^{(n)}\le\frac{1}{b_0^{(n)}}\le\frac{1}{2\kappa}$, one gets

$$\begin{aligned}w^n&\le 2w^0+2\kappa\sum_{k=1}^{n-1}w^k\sum_{j=k}^{n}(Q_d)_{n-j}^{(n)}\lambda^{j-k}+2\sum_{j=1}^{n}(Q_d)_{n-j}^{(n)}g^j\\&\le 2\kappa\sum_{k=1}^{n-1}w^k\sum_{j=k}^{n}\tau_j\lambda^{j-k}+2w^0+2\sum_{j=1}^{n}\frac{g^j}{b_0^{(j)}}\quad\text{for } 1\le n\le N.\end{aligned}$$

Note that

$$4\sum_{k=1}^{n-1}\sum_{j=k}^{n}\tau_j\lambda^{j-k}\le 4\sum_{j=1}^{n}\tau_j\sum_{k=1}^{j}\lambda^{j-k}\le\frac{4t_n}{1-\lambda}.$$

The desired result follows by the standard Grönwall inequality, and the proof is complete. ∎

We are now ready to present the following convergence result.

THEOREM 5.1. *Let the initial data u_0 be smooth and bounded by* 1*, and let the solution of* (2.1)–(2.2) *be sufficiently smooth. Assume that the step-ratio restriction* **S0** *holds and the time-step size satisfies* (4.13)*. The numerical solution u_h^n of the BDF*2 *scheme* (2.7) *is convergent in the maximum norm, and it holds that*

$$\left\|u(\mathbf{x}_h,t_n)-u_h^n\right\|_\infty\le\frac{C_u t_n}{1-\eta}\exp\left(\frac{4t_n}{1-\eta}\right)\left(\tau^2+h^2\right)\quad\textit{for } 1\le n\le N,$$

where the recombined parameter η is determined by (4.12)*, and C_u is a constant that is independent of the time-step sizes and time-step ratios.*

Proof. Let $U_h^n:=u(\mathbf{x}_h,t_n)$ and $e_h^n:=U_h^n-u_h^n\in\mathbb{V}_h$ for $\mathbf{x}_h\in\bar{\Omega}_h$ and $0\le n\le N$. It is easy to find that the exact solution U_h^n satisfies the governing equation

$$D_2U^n=\varepsilon^2\Lambda_hU^n-f(U^n)+\Upsilon^n+R^n,\quad 1\le n\le N,$$

where Υ^n and R^n denote the truncation errors in time and space, respectively. Subtracting the numerical scheme (2.7) from the above equation, one gets

$$D_2 e^n = \varepsilon^2 \Lambda_h e^n + f(u^n) - f(U^n) + \Upsilon^n + R^n, \quad 1 \le n \le N, \tag{5.4}$$

with $e^0 = 0$. As done before, we define $\bar{e}^k := e^k - \eta e^{k-1}$ for $k \ge 1$ with $\bar{e}^0 := e^0 = 0$. Recalling the elementary inequality

$$|(a^3 - a) - (b^3 - b)| \le 2|a - b| \quad \forall\, a, b \in [-1, 1],$$

we apply Theorem 4.1 (discrete maximum bound principle) to get

$$\big\|f(U^n) - f(u^n)\big\|_\infty \le 2\big\|e^n\big\|_\infty. \tag{5.5}$$

By using the alternative formulas (4.2)–(4.3), we rewrite the error equation (5.4) as

$$\sum_{j=1}^{n} d_{n-j}^{(n)} \nabla_\tau \bar{e}^j - \varepsilon^2 \sum_{j=1}^{n} \eta^{n-j} \Lambda_h \bar{e}^j = f(u^n) - f(U^n) + \Upsilon^n + R^n, \quad 1 \le n \le N,$$

or

$$\begin{aligned} \big(d_0^{(n)} - \varepsilon^2 \Lambda_h\big)\bar{e}^n = {} & \sum_{j=1}^{n-1} \big(d_{n-j-1}^{(n)} - d_{n-j}^{(n)} - \varepsilon^2 \eta^{n-j} \Lambda_h\big)\bar{e}^j \\ & + f(u^n) - f(U^n) + \Upsilon^n + R^n, \quad 1 \le n \le N. \end{aligned}$$

By applying Lemma 4.2 and the estimate (5.5), one gets

$$\begin{aligned} d_0^{(n)} \big\|\bar{e}^n\big\|_\infty \le {} & \big\|\big(d_0^{(n)} - \varepsilon^2 \Lambda_h\big)\bar{e}^n\big\|_\infty \\ \le {} & \sum_{j=1}^{n-1} \big\|\big(d_{n-j-1}^{(n)} - d_{n-j}^{(n)} - \varepsilon^2 \eta^{n-j} \Lambda_h\big)\bar{e}^j\big\| \\ & + 2\big\|e^n\big\|_\infty + \big\|\Upsilon^n\big\|_\infty + \big\|R^n\big\|_\infty, \quad 1 \le n \le N. \end{aligned}$$

Under the time-step constraint (4.13), Lemma 4.1 with $S_n = 0$ yields

$$\big\|\big(d_{n-j-1}^{(n)} - d_{n-j}^{(n)} - \varepsilon^2 \eta^{n-j} \Lambda_h\big)\bar{e}^j\big\|_\infty \le \big(d_{n-j-1}^{(n)} - d_{n-j}^{(n)}\big)\big\|\bar{e}^j\big\|_\infty, \quad 1 \le j \le n-1.$$

Thus, by applying the substitution formula (4.2) and the triangle inequality, it follows that

$$d_0^{(n)} \big\|\bar{e}^n\big\|_\infty \le \sum_{j=1}^{n-1} \big(d_{n-j-1}^{(n)} - d_{n-j}^{(n)}\big)\big\|\bar{e}^j\big\|_\infty + 2\sum_{j=1}^{n} \eta^{n-j} \big\|\bar{e}^j\big\|_\infty + \big\|\Upsilon^n\big\|_\infty + \big\|R^n\big\|_\infty,$$

or

$$\sum_{j=1}^{n} d_{n-j}^{(n)} \nabla_\tau \big\|\bar{e}^j\big\|_\infty \le 2\sum_{j=1}^{n} \eta^{n-j} \big\|\bar{e}^j\big\|_\infty + \big\|\Upsilon^n\big\|_\infty + \big\|R^n\big\|_\infty, \quad 1 \le n \le N.$$

Under the choice (4.12), one has $\eta \in [\frac{1}{2}, 1)$. It is easy to check that the time-step constraint (4.13) implies $\tau_n \le \frac{1+2r_n}{4(1+r_n)}$ or $b_0^{(n)} \ge 4$. So Lemma 5.1 with $\kappa = 2$ and $\lambda := \eta$ yields

$$\big\|\bar{e}^n\big\|_\infty \le 2\exp\left(\frac{4t_n}{1-\eta}\right) \sum_{j=1}^{n} \frac{1}{b_0^{(j)}} \left(\big\|\Upsilon^j\big\|_\infty + \big\|R^j\big\|_\infty\right) \quad \text{for } 1 \le n \le N.$$

Then the substitution formula (4.2) gives

$$\|e^n\|_\infty \le \frac{2}{1-\eta}\exp\left(\frac{4t_n}{1-\eta}\right)\sum_{j=1}^{n}\frac{1}{b_0^{(j)}}\left(\|\Upsilon^j\|_\infty + \|R^j\|_\infty\right) \quad \text{for } 1\le n\le N. \tag{5.6}$$

Obviously, $\|R^j\|_\infty \le C_u h^2$ for $j\ge 1$ and thus we have

$$\sum_{j=1}^{n}\frac{1}{b_0^{(j)}}\|R^j\|_\infty \le \sum_{j=1}^{n}\tau_j\|R^j\|_\infty \le C_u t_n h^2.$$

By the Taylor expansion (e.g., [27, Theorem 10.5]), one has $\Upsilon^1 = -\frac{1}{\tau_1}\int_{t_0}^{t_1} t\,\partial_{tt}u(t)\,\mathrm{d}t$ and

$$\Upsilon^n = -\frac{1+r_n}{2\tau_n}\int_{t_{n-1}}^{t_n}(t-t_{n-1})^2\partial_{ttt}u(t)\,\mathrm{d}t + \frac{r_n^2}{2(1+r_n)\tau_n}\int_{t_{n-2}}^{t_n}(t-t_{n-2})^2\partial_{ttt}u(t)\,\mathrm{d}t,\ n\ge 2.$$

We have $\|\Upsilon^1\|_\infty \le b_0^{(1)}\tau_1\int_{t_0}^{t_1}\|\partial_{tt}u(t)\|_\infty\,\mathrm{d}t$ and

$$\begin{aligned}
\|\Upsilon^j\|_\infty &\le \frac{1+r_j}{2}\tau_j\int_{t_{j-1}}^{t_j}\|\partial_{ttt}u(t)\|_\infty\,\mathrm{d}t + \frac{r_j^2(\tau_j+\tau_{j-1})^2}{2(1+r_j)\tau_j}\int_{t_{j-2}}^{t_j}\|\partial_{ttt}u(t)\|_\infty\,\mathrm{d}t\\
&= (1+r_j)\tau_j\int_{t_{j-1}}^{t_j}\|\partial_{ttt}u(t)\|_\infty\,\mathrm{d}t + \frac{\tau_j(1+r_j)}{2}\int_{t_{j-2}}^{t_{j-1}}\|\partial_{ttt}u(t)\|_\infty\,\mathrm{d}t\\
&= (b_0^{(j)}-b_1^{(j)})\tau_j^2\left(\int_{t_{j-1}}^{t_j}\|\partial_{ttt}u(t)\|_\infty\,\mathrm{d}t + \frac{1}{2}\int_{t_{j-2}}^{t_{j-1}}\|\partial_{ttt}u(t)\|_\infty\,\mathrm{d}t\right) \quad \text{for } j\ge 2,
\end{aligned}$$

where $b_0^{(j)}-b_1^{(j)} = (1+r_j)/\tau_j$ from the definition (2.9) has been used. It follows that

$$\begin{aligned}
\sum_{j=1}^{n}\frac{1}{b_0^{(j)}}\|\Upsilon^j\|_\infty &= \tau_1\int_{t_0}^{t_1}\|\partial_{tt}u(t)\|_\infty\,\mathrm{d}t + \sum_{j=2}^{n}\frac{1}{d_0^{(j)}}\|\Upsilon^j\|_\infty\\
&\le \tau_1\int_{t_0}^{t_1}\|\partial_{tt}u(t)\|_\infty\,\mathrm{d}t + \sum_{j=2}^{n}\left(1-b_1^{(j)}/b_0^{(j)}\right)\tau_j^2\int_{t_{j-1}}^{t_j}\|\partial_{ttt}u(t)\|_\infty\,\mathrm{d}t\\
&\quad + \frac{1}{2}\sum_{j=1}^{n-1}\left(1-b_1^{(j+1)}/b_0^{(j+1)}\right)r_{j+1}^2\tau_j^2\int_{t_{j-1}}^{t_j}\|\partial_{ttt}u(t)\|_\infty\,\mathrm{d}t\\
&\le \tau_1\int_{t_0}^{t_1}\|\partial_{tt}u(t)\|_\infty\,\mathrm{d}t + 8\sum_{j=1}^{n}\tau_j^2\int_{t_{j-1}}^{t_j}\|\partial_{ttt}u(t)\|_\infty\,\mathrm{d}t \quad \text{for } n\ge 1,
\end{aligned}$$

where the step-ratio restriction **S0** was applied. Therefore, we obtain from (5.6) that

$$\|e^n\|_\infty \le \frac{2}{1-\eta}\exp\left(\frac{4t_n}{1-\eta}\right)\left(\tau_1\int_{t_0}^{t_1}\|\partial_{tt}u(t)\|_\infty\,\mathrm{d}t + 8\sum_{j=1}^{n}\tau_j^2\int_{t_{j-1}}^{t_j}\|\partial_{ttt}u(t)\|_\infty\,\mathrm{d}t + C_u t_n h^2\right).$$

This completes the proof. ∎

6. Numerical implementations. In this section, we shall provide some details on the numerical implementations and present several numerical examples. For the nonlinear BDF2 scheme (2.7), we shall perform a simple Newton-type iteration procedure at each time level with a tolerance 10^{-12}. We always choose the solution at the previous level as the initial value of Newton iteration. For more advanced nonlinear solvers, one can refer to [5, 28, 30].

6.1. Adaptive time-stepping strategy. In simulating the phase field problems, the temporal evolution of phase variables involves multiple time scales, such as the coarsening dynamics problems discussed in Example 3, and an initial random perturbation evolves on a fast time scale while later dynamic coarsening evolves on a very slow time scale. Therefore, the adaptive time-stepping strategy is more practical to efficiently resolve widely varying time scales and to significantly reduce the computational cost. On the other hand, one remarkable advantage of the maximum norm stable scheme is that it can be easily combined with an adaptive time strategy, which adjusts the size of time step based on the accuracy requirement only. In this paper, we use Algorithm 1, which is motivated by [11], to choose adaptive time steps.

Algorithm 1 Adaptive time-stepping strategy.

Require: Given u^n and time step τ_n
1: Compute u_1^{n+1} by using first-order scheme with time step τ_n.
2: Compute u_2^{n+1} by using second-order scheme with time step τ_n.
3: Calculate $e_{n+1} = \|u_2^{n+1} - u_1^{n+1}\|/\|u_2^{n+1}\|$.
4: **if** $e_{n+1} < tol$ **then**
5: Update time-step size $\tau_{n+1} \leftarrow \min\{\max\{\tau_{\min}, \tau_{ada}\}, \tau_{\max}\}$.
6: **else**
7: Recalculate with time-step size $\tau_n \leftarrow \min\{\max\{\tau_{\min}, \tau_{ada}\}, \tau_{\max}\}$.
8: Goto 1
9: **end if**

The first-order and second-order schemes used in Algorithm 1 refer to the backward Euler method and the adaptive BDF2 scheme in this article, respectively. The adaptive time step τ_{ada} is given by

$$\tau_{ada} = \min\left\{2.414,\ \rho\left(\frac{tol}{e}\right)^{\frac{1}{2}}\right\}\tau_{cur},$$

in which ρ is a default safety coefficient, tol is a reference tolerance, e is the relative error at each time level, and τ_{cur} is the current time step. In addition, $\tau_{\max}$ and $\tau_{\min}$ are the predetermined maximum and minimum time steps. In our computation, if not explicitly specified, we choose $\rho = 0.6$, $tol = 10^{-4}$, $\tau_{\max} = 0.1$, and $\tau_{\min} = 10^{-3}$.

6.2. Numerical examples.

Example 1. To test the accuracy, we first consider $\partial_t u = \frac{1}{8\pi^2}\Delta u - f(u) + g(\mathbf{x}, t)$ for $\mathbf{x} \in (0,1)^2$ and $0 < t < 1$ such that it has an exact solution $u = \sin(2\pi x)\sin(2\pi y)\sin t$.

The numerical accuracy in time of the BDF2 scheme is examined by using the random mesh, that is, $\tau_k := T\epsilon_k/S$ for $1 \le k \le N$, where $S = \sum_{k=1}^{N} \epsilon_k$ and $\epsilon_k \in (0,1)$ are random numbers. The maximum norm error $e(N) := \max_{1\le n\le N} \|U^n - u^n\|_\infty$ is recorded in each run, and the experimental order of convergence is computed by

$$\text{Order} \approx \frac{\log\left(e(N)/e(2N)\right)}{\log\left(\tau(N)/\tau(2N)\right)},$$

where $\tau(N)$ denotes the maximum time-step size for a total of N subintervals. We take the spatial grid points $M_1 = 1024$ in each direction such that the temporal error dominates the spatial error in each run, and we solve the problem with $T = 1$. The numerical results are listed in Table 1, where the number of step ratios $r_k \ge 1 + \sqrt{2}$ is

also listed in the fifth column. It is somewhat surprising that the nonuniform BDF2 scheme on random meshes maintains second-order accuracy even when there exist large step ratios that do not satisfy the requirement $r_k < 1 + \sqrt{2}$.

TABLE 1
Numerical accuracy of BDF2 scheme at time $T = 1$.

N	τ	$e(N)$	Order	$r_k \geq 1 + \sqrt{2}$
10	1.88e-01	2.56e-03	–	1
20	1.10e-01	8.16e-04	2.12	4
40	4.67e-02	1.39e-04	2.06	3
80	2.42e-02	3.41e-05	2.14	9

Example 2. We next consider the Allen–Cahn model (2.1)–(2.2) with the diffusion coefficient $\varepsilon = 0.02$. The nonuniform BDF2 scheme is applied to simulate the merging of four bubbles with an initial condition

$$\begin{aligned}\phi_0(\mathbf{x}) = &-\tanh\left(\left((x-0.3)^2+y^2-0.2^2\right)/\varepsilon\right)\tanh\left(\left((x+0.3)^2+y^2-0.2^2\right)/\varepsilon\right)\\ &\times\tanh\left(\left(x^2+(y-0.3)^2-0.2^2\right)/\varepsilon\right)\tanh\left(\left(x^2+(y+0.3)^2-0.2^2\right)/\varepsilon\right).\end{aligned} \tag{6.1}$$

The computational domain $\Omega = (-1, 1)^2$ is divided uniformly into 128 parts in each direction.

We now examine different time strategies, i.e., the uniform and adaptive time approaches, for simulating the merging of four bubbles. We start with the calculation of the solution until the time $T = 30$ with a constant time step $\tau = 10^{-3}$. We then implement the adaptive strategy described in Algorithm 1 to simulate the merging of bubbles. The time evolution of discrete energies and time steps are depicted in Figure 1. As can be seen, the adaptive energy curve is practically indistinguishable from the one obtained using the small constant time step $\tau = 10^{-3}$. As a consequence, the total number of adaptive time steps is 511, while it takes 30,000 steps for the uniform grid, showing that the time-stepping adaptive strategy is computationally efficient.

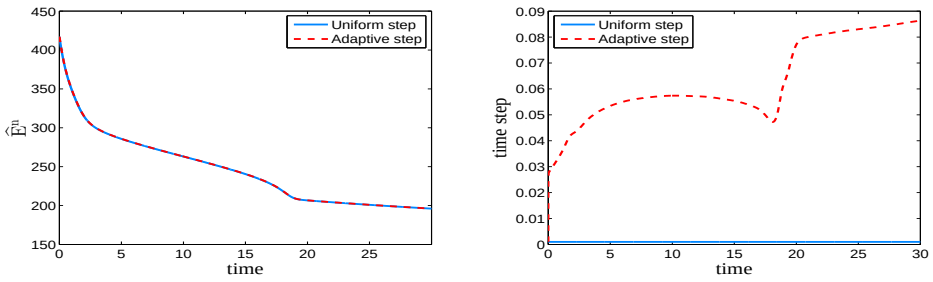

FIG. 1. *Evolutions of energy (left) and time steps (right) of the Allen–Cahn equation using different time strategies until time $T = 30$.*

We now apply the nonuniform BDF2 scheme coupled with the adaptive time strategy to simulate the merging of bubbles with $T = 100$. The time evolution of the phase variable is summarized in Figure 2. As can be seen in the figures, the initial separated four bubbles gradually coalesce into a single big bubble, while the volume becomes smaller with time owing to the fact that the Allen–Cahn model does not

conserve the initial volume. The discrete energy and adaptive time step are shown in Figure 3. We observe that the energy evolution undergoes large variations initially and at time $t = 20$ but changes very little in other time intervals. As a result, we see that small time steps are used when the energy variation is large, while large time steps are utilized when the energy variation is small.

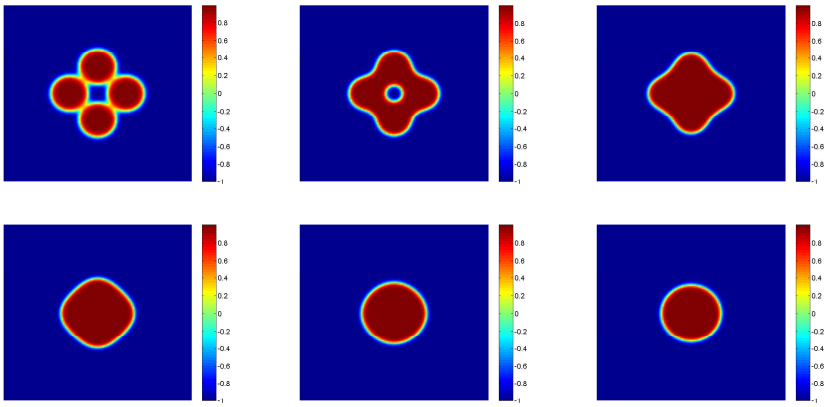

FIG. 2. *Solution snapshots of the Allen–Cahn equation using the adaptive time strategy at* $t = 1, 10, 20, 50, 80, 100$, *respectively.*

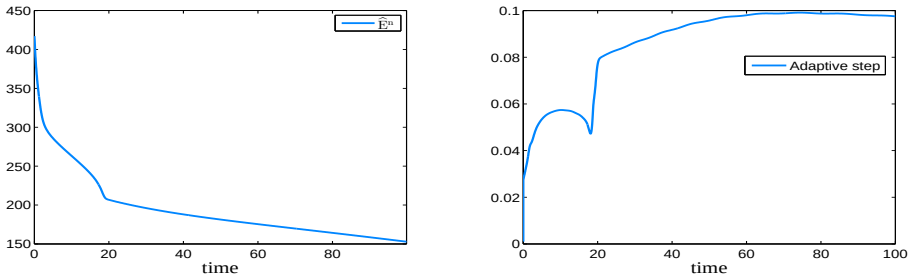

FIG. 3. *Evolutions of energy (left) and time steps (right) of the Allen–Cahn equation using the adaptive time strategy until final time* $T = 100$.

Example 3. We finally consider the coarsening dynamics of the Allen–Cahn model with the model parameter $\varepsilon = 0.01$. We choose a random initial condition $u_0 = 0.95 + rand(\mathbf{x}) \times 0.05$ by assigning a random number varying from -0.05 to 0.05 at each grid point. In the following computation, we use 128×128 uniform meshes in space to discretize the domain $\Omega = (0, 1)^2$.

We first investigate the effect of uniform time-step size on the maximum norm and discrete energy. The numerical results obtained from different time steps $\tau = 0.2, 0.4, 0.8$ with $T = 100$ are shown in Figure 4. As can be seen from the figures, the maximum values of the numerical solutions are bounded by 1 and the energy dissipation law holds if time steps $\tau = 0.2, 0.4$. These numerical results imply that the constraint (4.13) for the time-step size to ensure the discrete maximum bound principle is a sufficient condition.

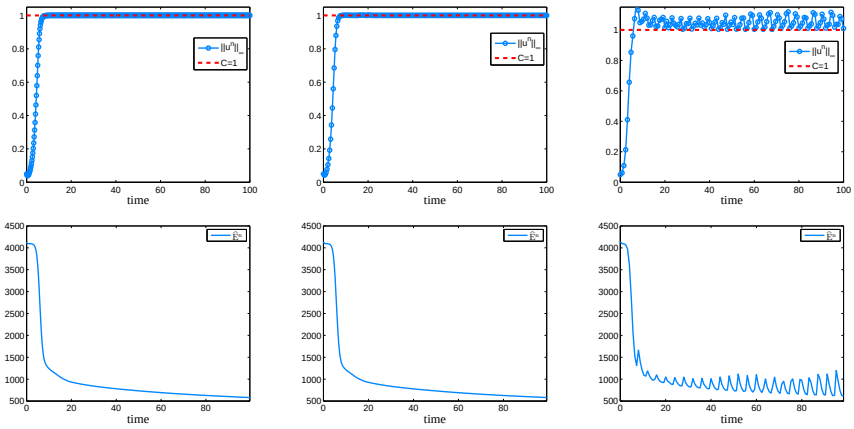

FIG. 4. *Maximum norm (top) and energy (bottom) of the Allen–Cahn equation using different time steps* $\tau = 0.2, 0.4, 0.8$ *(from left to right), respectively.*

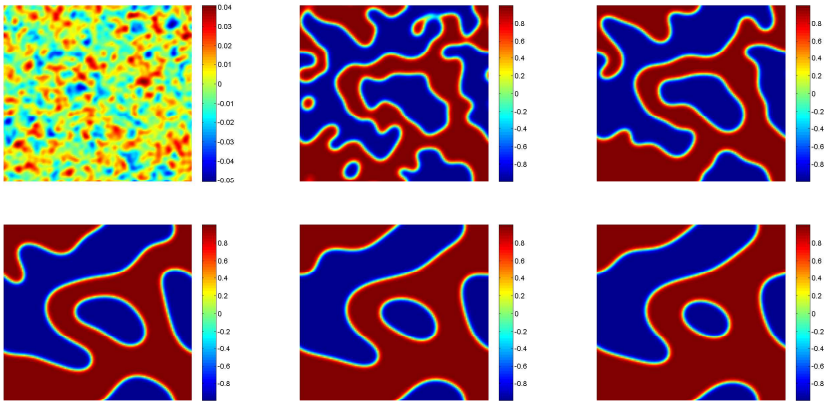

FIG. 5. *Solution snapshots of coarsening dynamics of the Allen–Cahn equation using the adaptive time strategy at* $t = 1, 10, 20, 50, 80, 100$*, respectively.*

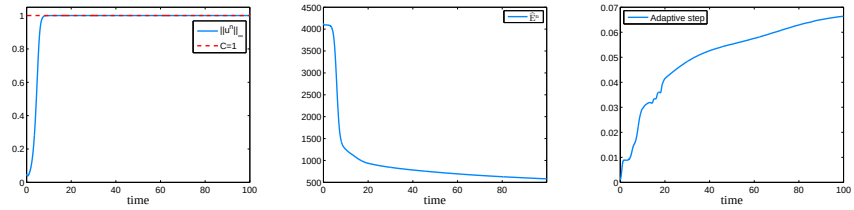

FIG. 6. *Evolutions of maximum norm (left), energy (middle), and adaptive time steps (right) of coarsening dynamics of the Allen–Cahn equation using the adaptive time strategy.*

We next investigate the coarsening dynamic of the Allen–Cahn model by using the adaptive BDF2 scheme incorporated with the adaptive algorithm until $T = 100$. Figure 5 shows the time evolution of the coarsening dynamic. As can be seen at $t = 1$, the microstructure is relatively fine and contains a large number of grains.

As time evolves, the coarsening dynamic through migration of the phase boundaries, decomposition, and merging procedure can be observed. Also, as a consequence the number of grains becomes smaller with time. The corresponding discrete maximum norm, energy, and adaptive time step are plotted in Figure 6, where we observe that the maximum value of the numerical solutions is bounded by 1, the discrete energy decays monotonically, and the adaptive strategy is rather effective.

7. Concluding remarks. This work is concerned with fully discretized numerical schemes for the Allen–Cahn equations. The main task of this work is to establish the energy stability, maximum bound principle, and convergence analysis for the second-order BDF scheme with variable time steps. It is of practical importance to allow the use of variable time steps as the solutions of the Allan–Cahn equations may undergo different time regimes and require fine or coarse time steps accordingly. Of course, the ratio of the meshsize may increase or decrease smoothly in order to retain numerical stability. Consequently, some upper bounds may apply in the practical computations.

In this work, by using an appropriate energy method we have shown that the nonuniform BDF2 scheme preserves the energy dissipation law under a mild time-ratio constraint. By using a kernels recombination and complement technique, we show that the discrete maximum bound principle holds for the nonuniform BDF2 scheme under the time-ratio constraint $r_k < 1 + \sqrt{2}$, which coincides with the Grigorie zero-stability condition. This maximum-principle preserving result seems very new for second-order time discretizations to the Allen–Cahn equation. This discrete maximum bound principle allows us to obtain the error estimates without any Lipschitz assumptions on the nonlinear bulk force. With the use of the KRC technique and a new Gronwall inequality, the second-order rate of convergence in the maximum norm is finally established.

It is expected that the KRC technique developed in this work can be used to deal with more general nonlinear problems. One challenging topic is to develop nonuniform BFD2-type schemes for the time-fractional phase field equations [19, 26]. As the time-fractional operators require solution information at all time levels, the use of variable time steps seems more important in practice. On the technical side, it is of interest to see whether the ratio constraints **S1** and **S0** are optimal or not.

Acknowledgment. The authors would like to thank Dr. Bingquan Ji for his kind help with numerical simulations.

REFERENCES

[1] M. Allen and W. Cahn, *A microscopic theory for antiphase boundary motion and its application to antiphase domain coarsening*, Acta Metall., 27 (1979), pp. 1085–1095.

[2] J. Becker, *A second order backward difference method with variable steps for a parabolic problem*, BIT, 38 (1998), pp. 644–662.

[3] J. Cahn and J. Hilliard, *Free energy of a nonuniform system* I. *Interfacial free energy*, J. Chem. Phys., 28 (1958), pp. 258–267.

[4] W. Chen, X. Wang, Y. Yan, and Z. Zhang, *A second order BDF numerical scheme with variable steps for the Cahn–Hilliard equation*, SIAM J. Numer. Anal., 57 (2019), pp. 495–525, https://doi.org/10.1137/18M1206084.

[5] W. Chen, C. Wang, X. Wang, and S. Wise, *A linear iteration algorithm for energy stable second order scheme for a thin film model without slope selection,* J. Sci. Comput., 59 (2014), pp. 574–601.

[6] Q. Du, L. Ju, X. Li, and Z. Qiao, *Maximum principle preserving exponential time differencing schemes for the nonlocal Allen–Cahn equation,* SIAM J. Numer. Anal., 57 (2019), pp. 875–898, https://doi.org/10.1137/18M118236X.

[7] E. Emmrich, *Stability and error of the variable two-step BDF for semilinear parabolic problems*, J. Appl. Math. Comput., 19 (2005), pp. 33–55.
[8] X. Feng, T. Tang, and J. Yang, *Long time numerical simulations for phase-field problems using p-adaptive spectral deferred correction methods,* SIAM J. Sci. Comput., 37 (2015), pp. A271–A294, https://doi.org/10.1137/130928662.
[9] C. W. Gear and K. W. Tu, *The effect of variable mesh size on the stability of multistep methods*, SIAM J. Numer. Anal., 11 (1974), pp.1025–1043, https://doi.org/10.1137/0711079.
[10] R. D. Grigorieff, *Stability of multistep-methods on variable grids*, Numer. Math., 42 (1983), pp. 359–377.
[11] H. Gomez and T. J. Hughes, *Provably unconditionally stable, second-order time-accurate, mixed variational methods for phase-field models*, J. Comput. Phys., 230 (2011), pp. 5310–5327.
[12] Y. He, Y. Liu, and T. Tang, *On large time-stepping methods for the Cahn-Hilliard equation,* Appl. Numer. Math., 57 (2006), pp. 616–628.
[13] A. Hawkins-Daarud, K. G. Van Der Zee, and J. T. Oden, *Numerical simulation of a thermodynamically consistent four-species tumor growth model.* Internat. J. Numer. Methods Biomed. Engrg., 8 (2012), pp. 3–24.
[14] T. Hou, T. Tang, and J. Yang, *Numerical analysis of fully discretized Crank-Nicolson scheme for fractional-in-space Allen-Cahn equations*, J. Sci. Comput., 72 (2017), pp. 1–18.
[15] M.-N. Le Roux, *Variable step size multistep methods for parabolic problems*, SIAM J. Numer. Anal., 19 (1982), pp. 725–741, https://doi.org/10.1137/0719051.
[16] Y. Li, Y. Choi, and J. Kim, *Computationally efficient adaptive time step method for the Cahn-Hilliard equation*, Comput. Math. Appl., 73 (2017), pp. 1855–1864.
[17] H.-L. Liao, D. Li, and J. Zhang, *Sharp error estimate of nonuniform L1 formula for linear reaction-subdiffusion equations*, SIAM J. Numer. Anal., 56 (2018), pp. 1112–1133, https://doi.org/10.1137/17M1131829.
[18] H.-L. Liao, W. McLean, and J. Zhang, *A discrete Grönwall inequality with applications to numerical schemes for subdiffusion problems*, SIAM J. Numer. Anal., 57 (2019), pp. 218–237, https://doi.org/10.1137/16M1175742.
[19] H.-L. Liao, T. Tang, and T. Zhou, *A second-order and nonuniform time-stepping maximum-principle preserving scheme for time-fractional Allen-Cahn equations,* J. Comput. Phys., 414 (2020), 109473.
[20] F. Lou, T. Tang, and H. Xie, *Parameter-free time adaptivity based on energy evolution for the Cahn-Hilliard equation,* Commun. Comput. Phys., 19 (2016), pp. 1542–1563.
[21] L. Ma, R. Chen, X. Yang, and H. Zhang, *Numerical approximations for Allen-Cahn type phase field model of two-phase incompressible fluids with moving contact lines,* Commun. Comput. Phys., 27 (2017), pp. 867–889.
[22] H. Nishikawa, *On large start-up error of BDF*2, J. Comput. Phys., 392 (2019), pp. 456–461.
[23] Z. Qiao, Z. Zhang, and T. Tang, *An adaptive time-stepping strategy for the molecular beam epitaxy models*, SIAM J. Sci. Comput., 33 (2011), pp. 1395–1414, https://doi.org/10.1137/100812781.
[24] J. Shen and X. Yang, *Numerical approximations of Allen-Cahn and Cahn-Hilliard equations,* Discrete Contin. Dyn. Syst., 28 (2010), pp. 1669–1691.
[25] J. Shen, X. Yang, and H. Yu, *Efficient energy stable numerical schemes for a phase field moving contact line model,* J. Comput. Phys., 284 (2015), pp. 617–630.
[26] T. Tang, H. Yu, and T. Zhou, *On energy dissipation theory and numerical stability for time-fractional phase field equations,* SIAM J. Sci. Comput., 41 (2019), pp. A3757–A3778, https://doi.org/10.1137/18M1203560.
[27] V. Thomée, *Galerkin Finite Element Methods for Parabolic Problems*, 2nd ed., Springer-Verlag, New York, 2006.
[28] C. Wang, X. Wang, and S. Wise, *Unconditionally stable schemes for equations of thin film epitaxy,* Discrete Contin. Dyn. Syst. Ser. A, 28 (2010), pp. 405–423.
[29] S. M. Wise, J. S. Lowengrub, H. B. Frieboes, and V. Cristini, *Three-dimensional multispecies nonlinear tumor growth* I: *Model and numerical method,* J. Theoret. Biol., 253 (2008), pp. 524–543.
[30] Y. Yan, W. Chen, C. Wang, and S. M. Wise, *A second-order energy stable BDF numerical scheme for the Cahn-Hilliard equation,* Commun. Comput. Phys, 23 (2018), pp. 572–602.
[31] Z. Zhang, Y. Ma, and Z. Qiao, *An adaptive time-stepping strategy for solving the phase field crystal model*, J. Comput. Phys., 249 (2013), pp. 204–215.